Morphological and molecular evidence supports specific recognition of the recently extinct *Bettongia anhydra* (Marsupialia: Macropodidae)

Matthew C. McDowell,* Dalal Haouchar, Ken P. Aplin, Michael Bunce, Alexander Baynes and Gavin J. Prideaux

School of Biological Sciences, Flinders University, Bedford Park, Adelaide, South Australia 5042, Australia (MCM, GJP)
Trace and Environmental DNA (TrEnD) Laboratory, Department of Environment and Agriculture, Curtin University, Perth, Western Australia 6102, Australia (DH, MB)
Division of Mammals, Smithsonian Institution, PO Box 37012, MRC 108, Washington, DC 20013-7012, USA (KPA)
Department of Earth and Planetary Sciences, Western Australian Museum, Locked Bag 49, Welshpool DC, Western Australia 6986, Australia (AB)

* Correspondent: matthew.mcdowell@flinders.edu.au

In 1933, geologist and explorer Michael Terry collected the skull of a small macropodid captured by members of his party near Lake Mackay, western Northern Territory. In 1957, this skull was described as the sole exemplar of a distinct subspecies, *Bettongia penicillata anhydra*, but was later synonymized with *B. lesueur* and thereafter all but forgotten. We use a combination of craniodental morphology and ancient mitochondrial DNA to confirm that the Lake Mackay specimen is taxonomically distinct from all other species of *Bettongia* and recognize an additional specimen from a Western Australian Holocene fossil accumulation. *B. anhydra* is morphologically and genetically most similar to *B. lesueur* but differs in premolar shape, rostrum length, dentary proportions, and molar size gradient. In addition, it has a substantial mitochondrial cytochrome *b* pairwise distance of 9.6–12% relative to all other bettongs. The elevation of this recently extinct bettong to species status indicates that Australia's mammal extinction record over the past 2 centuries is even worse than currently accepted. Like other bettongs, *B. anhydra* probably excavated much of its food and may have performed valuable ecological services that improved soil structure and water infiltration and retention, as well as playing an important role in the dispersal of seeds and mycorrhizal fungal spores. All extant species of *Bettongia* have experienced extensive range contractions since European colonization and some now persist only on island refugia. The near total loss of these ecosystem engineers from the Australian landscape has far-reaching ecological implications.

Key words: biodiversity loss, digging, ecological service, environmental degradation, extinction

European colonization has had major environmental repercussions that have fundamentally transformed Australia's biogeography, ecosystems, and landscapes, causing widespread declines in biodiversity (e.g., McDowell et al. 2012). While these impacts have affected all Australian native mammals, few taxa have fared as badly as the potoroines (species of *Aepyprymnus*, *Bettongia*, *Caloprymnus* and *Potorous*)—van Dyck and Strahan (2008). Potoroines typically excavate the majority of their food, and in doing so, perform valuable ecosystem services such as seed and spore dispersal, facilitation of seedling germination and establishment, soil aeration, incorporation of organic matter, and improvement in moisture infiltration (Martin 2003; Fleming et al. 2013). Some exotic species such as rabbits are also fossorial but do not contribute to soil improvement as effectively as potoroines (Vitousek 1990;

James et al. 2011). Consequently, in areas where Potoroines have been extirpated or become extinct, soils are likely to have become drier, dustier, more compacted, and less fertile, reducing the productivity of the whole ecosystem.

Potoroines, sometimes known as rat-kangaroos, are small- to medium-sized nocturnal marsupials that occupy a basal branch within the Macropodidae (Prideaux and Warburton 2010). They retain plesiomorphic characteristics such as a prehensile tail, less-reduced forelimbs, well-developed upper canines, large blade-like sectorial premolars, and low-crowned molars (Claridge et al. 2007). Many species of *Bettongia* subsist primarily on excavated hypogeal fungi (Seebeck and Rose 1989; Claridge et al. 2007), which form mycorrhizal associations with the roots of vascular plants and help to maintain soft, friable, well-structured topsoil (Martin 2003; Eldridge and James

2009; Eldridge et al. 2012). Bettongs were once broadly distributed across Australia, but since European colonization each species has been extirpated from much of their former ranges or have become extinct (Short 1998; van Dyck and Strahan 2008).

Four extant and 2 extinct species of *Bettongia* are currently recognized. Taxonomy of the genus was partially revised by Finlayson (1958) and more comprehensively by Wakefield (1967), who raised *B. tropica* from what had hitherto been considered a northern population of *B. penicillata*. Subsequently, 2 fossil species have been added: *B. moyesi* from the Miocene Riversleigh assemblage in northwestern Queensland (Flannery and Archer 1987) and *B. pusilla* from Holocene cave deposits of the Nullarbor Plain (McNamara 1997).

In describing *B. p. anhydra*, Finlayson (1957:553) noted its "remarkable blend of *penicillata* and *lesueuri* [sic] characters" and commented that "if its dual character were confirmed in series, it [*B. p. anhydra*] would merit specific recognition." Wakefield (1967) considered key features of the specimen, including its short rostrum, very large bullae, and proportionately long premolars, resembled *B. lesueur*, and thence declared them synonymous. One author (KPA) examined the holotype of *B. p. anhydra* in 1997 and concluded that it was specifically distinct. More recently, MCM independently reached the same conclusion and observed a Holocene fossil specimen from a Western Australian cave accumulation that demonstrates similar craniodental morphology. In this paper, we recognize *B. anhydra* as a distinct species on the basis of morphological and molecular evidence and consider the ecological implications of its 20th century disappearance.

Materials and Methods

Morphological analysis.—The holotype of *B. anhydra* (SAM M3582) was examined and compared with representative specimens of other species of *Bettongia* to determine taxonomic affinities. The following abbreviations are used in this work: FUR = Flinders University of South Australia reference collection; SAM = South Australian Museum (M: mammal collection; P: palaeontological collection); WAM = Western Australian Museum palaeontological collection; QM = Queensland Museum mammal collection. Dental homology, nomenclature, and family-group taxonomy follows Prideaux (2004) and Prideaux and Warburton (2010). Specimens used for comparison with *B. anhydra* are listed in Appendix I.

Genetic analysis.—The left turbinal bone from the nasal cavity of the *B. anhydra* holotype cranium was sampled using sterile forceps then placed in a labeled sterile vial. The turbinal was chosen because, being inside the nasal cavity, it has been largely protected from contamination due to human handling and its removal did not appreciably alter the appearance of the skull (see Wisely et al. 2004). DNA extraction procedures were carried out in a dedicated ancient DNA (aDNA) laboratory at Murdoch University, minimizing contamination from PCR amplicons and modern DNA. The sample was crushed to powder then stored for DNA extraction and amplification.

The bone digest buffer consisted of: 20 mM Tris pH 8.0 (Sigma, Kansas City, Missouri), 10 mM dithiothreitol (Thermo Fisher Scientific, Waltham, Massachusetts), 1 mg/ml proteinase K powder (Amresco, Solon, Ohio), 0.48 M ethylenediaminetetraacetic acid (Invitrogen, Carlsbad, California), and 1% Triton X-100 (Invitrogen). A total of 1,500 μl of bone digest buffer was added to the bone powder then incubated overnight at 55°C with rotation. After digestion, the solution was centrifuged at $13,000 \times g$ for 1 min to pellet undigested material. The supernatant containing the DNA was concentrated to approximately 100 μl in a Vivaspin 500 column (MWCO 30,000; Sartorius Stedim Biotech, Goettingen, Germany) at $13,000 \times g$ then combined with 5 volumes of PBi buffer (Qiagen, Valencia, California). DNA was immobilized on silica spin columns (Qiagen) and washed with 700 μl of AW1 and AW2 wash buffers (Qiagen). Finally, the DNA was eluted from the silica in 50 μl of 10 mM Tris pH 8.0 (Sigma).

The DNA extract was screened using specifically designed primer sets targeting the cytochrome *b* gene for *Bettongia*. Primer sets woylie_cytb_139F ACCTTCCAACATTTGAGCCTGATG and woylie_cytb_388R TGAGCCGTAGTAGATTCCTC were used to target a ~ 200 base pair region of cytochrome *b* DNA. Each quantitative polymerase chain reaction (qPCR) was made up to a total volume of 25 μl, containing 12.5 μl ABI Power SYBR master mix (Applied Biosystems, Waltham, Massachusetts), 0.4 μM of forward and reverse primer, 8.5 μM H_2O, and 2 μl DNA extract. Reaction conditions for the specific mammal primer sets were as follows; heat denatured at 95°C for 5 min, followed by 50 cycles of 95°C for 30 s and 56°C for 30 s.

Once initial qPCR screening showed that DNA of sufficient quality and free of inhibition was achieved, it was prepared for Sanger sequencing. To ensure validity of DNA sequences and to overcome ancient DNA damage, multiple sequence data sets were created and an overall consensus was drawn for use in the final analyses. Amplicons were cleaned (Qiagen columns) and prepared for capillary sequencing following Haouchar et al. (2013). Alignments of nucleotide sequences were carried out in GENEIOUS 6.0.1 (Drummond et al. 2011), with any ambiguities resolved by eye. Other *Bettongia* sp. sequences provided by the National Center for Biotechnology Information's GenBank were used to construct an alignment of the new *B. anhydra* sequence, presented in the Bayesian phylogeny.

Phylogenetic analysis was estimated using the Bayesian phylogenetic program BEAST version 1.7.4 (Drummond and Rambaut 2007; Drummond et al. 2012). Sequences were run through JMODELTEST to determine the most appropriate nucleotide substitution model (Posada 2008). A relaxed uncorrelated log-normal clock was employed. Three independent runs of 1×10^6 generations were performed, with every 1,000 generations sampled with 10% burn-in. Analyses were checked in TRACER (Rambaut and Drummond 2009) for convergence and adequate effective sample size. Phylogenetic trees were summarized using TREEANNOTATER version 1.7.4 (Drummond and Rambaut 2007) and visualized in FIGTREE 1.4.0 (Rambaut 2007). The cytochrome *b* gene for *B. anhydra* has been deposited into GenBank under accession number KM974728.

RESULTS

Higher Systematics

Order Diprotodontia Owen, 1866
Superfamily Macropodoidea Gray, 1821
Family Macropodidae Gray, 1821
Subfamily Potoroinae Gray, 1821
Tribe Bettongini Flannery and Archer, 1987
Genus *Bettongia* Gray, 1837

Revised Diagnosis of Bettongini

Tribe Bettongini includes species of *Bettongia*, *Caloprymnus*, *Aepyprymnus*, and *Milliyowi*. Bettongins can be differentiated from members of the tribe Potoroini (containing *Potorous*) based on the following characters: cranium bears postglenoid process and discrete periotic ectotympanic process; I3 short crowned. P3 bears many fine vertical ridgelets; buccal crests of upper molars better developed than lingual counterparts; dentary stout with convex ventral margin; i1 lacks a dorsal and ventral enamel flange; p3 bears many vertical ridgelets; lingual crests of lower molars better developed than buccal counterparts.

Revised Diagnosis of Bettongia

Species of *Bettongia* are united by 1 synapomorphy: jugal extends dorsally to at least level of large lachrymal foramen. However, they can be further differentiated from species of *Caloprymnus* and *Aepyprymnus* by their combined possession of large posterior palatal vacuities, inflated auditory bullae, and P3/p3 with 6 or more vertical ridgelets.
Bettongia anhydra—Finlayson, 1957
Synonyms
Bettongia penicillata anhydra Finlayson, 1957
Bettongia penicillata anhydra Finlayson, 1958
Bettongia lesueur Wakefield, 1967; in part
Bettongia lesueur Calaby and Richardson, 1988; in part

Holotype

Near-complete adult cranium (SAM M3582) with associated left and right dentaries collected from a fresh carcass by Michael Terry in 1933 from the McEwin Hills area, near Lake Mackay, Northern Territory. Cranium lacks the entire occipital complex, both petrosals and ectotympanics, interparietal and part of the left squamosal; the tympanic bullae are broken but enough is preserved to infer shape and degree of inflation. Left dentary complete, though m4 absent. Right dentary articular process not preserved.

Type Locality

McEwin Hills, Lake MacKay area, Northern Territory, approximately 22°02′S, 129°47′E (Fig. 1).

Referred Specimens

Stegamite Cave (5N194), Eucla Basin: WAM 67.10.530, adult left maxilla with P3 and M1–3 (M4 absent). Note: this specimen was referred to *B. anhydra* based on morphological characters only.

Diagnosis

Bettongia anhydra can be distinguished from all other species of *Bettongia* by the following features: steep posterior molar gradient (M/m1 ≤ M/m2 > M/m3 >> M/m4) and highly reduced fourth molars (Table 1); anteroposterior compression of rostrum; marked interorbital constriction; and obscuration of m4, m3 hypolophid, and part of m3 protolophid by ascending ramus in lateral view.

It can be further separated from *B. gaimardi*, *B. penicillata*, and *B. tropica* by its greater degree of inflation of auditory bullae (similar to *B. lesueur*); from *B. pusilla* by its lower-crowned and less lophodont molars, and steeper molar gradient; from *B. gaimardi*, *B. lesueur*, *B. moyesi*, *B. pusilla*, and *B. tropica* by its greater buccal flexion of anterior third of P3; from *B. penicillata* by its lesser buccal flexion of anterior third of P3. Dentary differs from *B. gaimardi*, *B. lesueur*, *B. penicillata*, and *B. pusilla* in robustness of horizontal ramus and anterior occurrence of digastric eminence; from *B. gaimardi*, *B. moyesi*, *B. penicillata*, *B. pusilla*, and *B. tropica* in greater length and breadth of coronoid process and more acute angle between ascending ramus and horizontal ramus.

Morphological Analysis

All features in referred specimen are as for holotype. No juvenile or postcranial specimens are known.

Cranium.—Premaxilla short, with upright portion essentially vertical. Anterior edge of premaxilla very slightly arcuate in lateral view (Figs. 2a and 2e). Diastema very short, straight, and only slightly deflected anteroventrally relative to cheek tooth row; maxilla contributes to most of diastema length. I1 high crowned and peg shaped, I2 and I3 comparatively elongate anteroposteriorly. C1 well developed and close to, but shorter than I3. Anterior palatal foramina broad and short, terminating posteriorly just
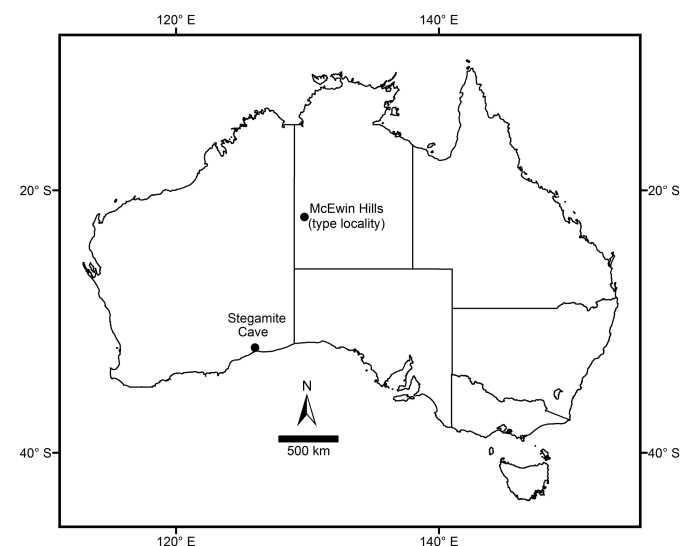

Fig. 1.—Collection locations of the holotype and referred specimen of *Bettongia anhydra*.

Table 1.—Mean cranial and dental measurements (mm) of modern *Bettongia* species. Some data for *B. gaimardi cuniculus*, *B. gaimardi gaimardi*, *B. penicillata ogilbyi*, and *B. tropica* after Wakefield (1967) and data for *B. lesueur* after Finlayson (1958).

|	*B. anhydra* (holotype)	WAM 67.10.530	*B. gaimardi cuniculus*	*B. gaimardi gaimardi*	*B. lesueur*	*B. penicillata ogilbyi*	*B. tropica*
Basal length			70.6	64.4	57.2	66.5	64.2
Zygomatic width	37.4		45.3	42.2	43.0	24.2	41.2
Interorbital width	12.2		19.9	18.5	14.5	17.4	15.8
Nasals length	23.7		34.7	30.8	26.3	32.5	29.6
Nasals, greatest width	9.5		14.5	13.9	12.8	13.5	13.5
Rostrum width	13.5		17.4	15.4	17.9	16	14.3
Nasal opening width	5.1		9.1	8.7	6.8	7.9	7.8
Bulla length	10.4		12.5	12.1	15.9	14.2	13.8
Bulla depth			9.5	9.1		10.6	10.9
P3 length	7.5	6.8	8.1	7.2	8.5	7.3	8.3
M1–3 length	10.5	10.6	13.7	12.8	11.7	12.4	13.2
M4 length	1.4		3.8	3.3	2.5	2.6	2.8
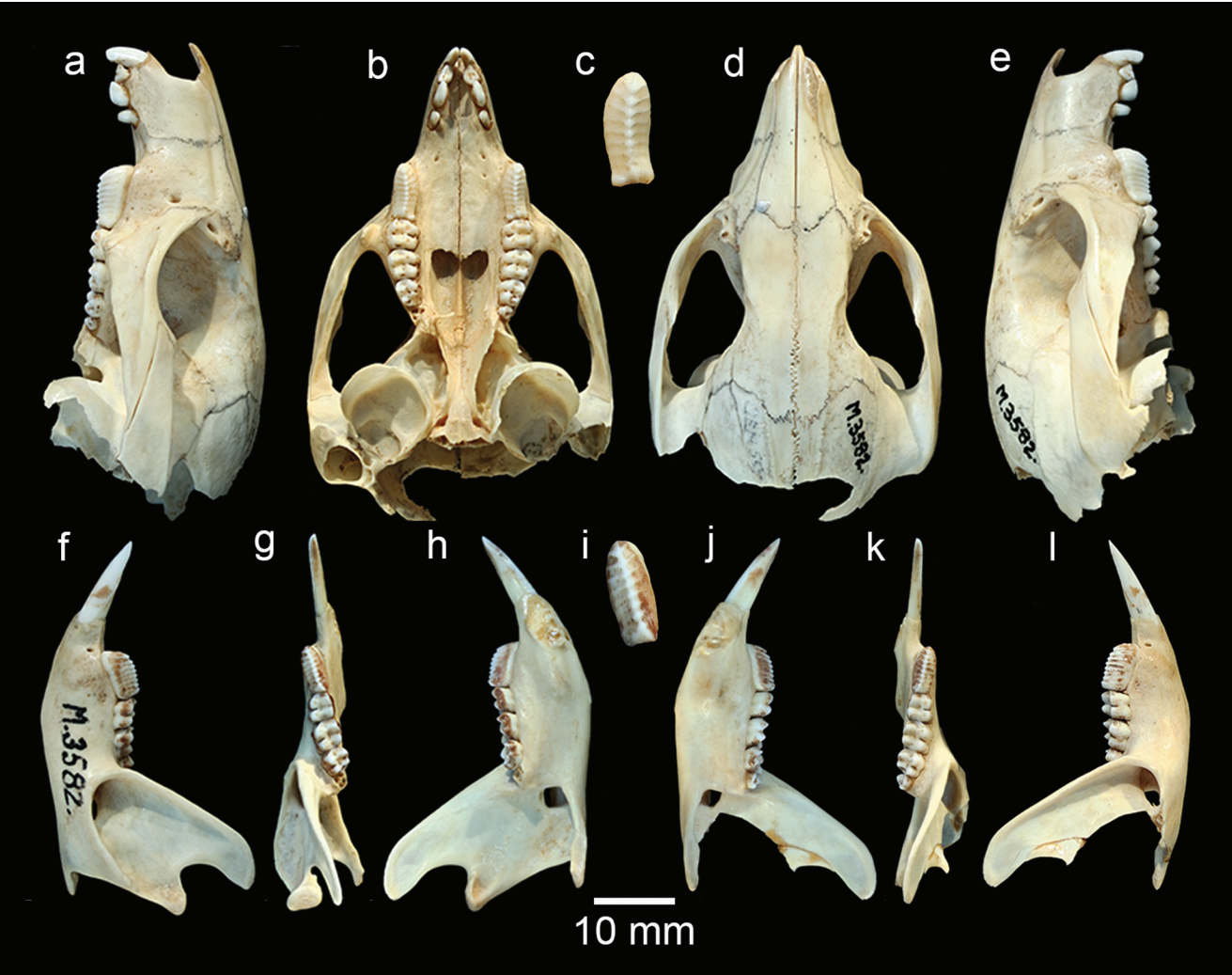
Fig. 2.—The holotype of *Bettongia anhydra* (SAM M3582): a) Left lateral, b) occlusal, c) magnified (2×) view of left P3, d) dorsal, e) right lateral aspect of skull, f) buccal, g) occlusal, h) lingual aspect of left dentary, i) magnified (2×) view of left p3, j) buccal, k) occlusal, l) lingual aspect of right dentary.

past anterior edge of C1 alveolus (Fig. 2b). Very short, deep rostrum strongly tapered anteriorly; lateral edges enclose angle of 20° (Figs. 2b and 2d). Premaxilla contributes approximately half of length of lateral surface of rostrum. Narial aperture deeper than wide (Figs. 2a and 2e). Buccinator fossa shallow, restricted to ventral half of lateral surface of rostrum and extending from

anterior edge of P3 anterior root to posterior edge of C1 alveolus (Figs. 2a, 2b, and 2d). Short masseteric process composed entirely of maxilla; positioned adjacent to M1 protoloph (Figs. 2a, 2b, and 2e). Infraorbital foramen opens anteriorly; positioned directly above posterior root of P3 at level of ventral border of orbit. Small posterior (dorsal) lacrimal foramen opens dorsally;

separated from larger anterior (ventral) lacrimal foramen by large lacrimal tuberosity which marks anterodorsal extremity of orbital rim. Anterior nasals narrowly constricted at maxilla–premaxilla suture. Nasofrontal sutures arcuate, extending posterior to anterior edge of orbit. Palatine bones well developed. Large posterior palatal foramina originate adjacent to metaloph of M1 and extend posteriorly along remaining length of palate (Fig. 2b).

Weakly developed temporal (parietal) crests confluent anteriorly with supraorbital crests, extending posteriorly across interparietals (Fig. 2d). Dorsal surface of neurocranium gently curved to posterior terminus of nasals. Zygomatic arch deep; posterior extremity of jugal bears very small ectoglenoid process (Figs. 2a and 2d). Postorbital process of jugal distinct and pointed. Zygomatic process of squamosal arises well anterior of occiput. Very small postglenoid process forms posterior border of glenoid fossa, curves slightly anteriorly at extremity, giving glenoid fossa a semicircular shape when viewed laterally. Auditory bullae highly inflated (Fig. 2b).

Upper incisors.—I1 high crowned, arcuate when viewed laterally (Figs. 2a and 2e). I2 blade like, crown height lower than I3. I3 crown subtriangular in buccal view (Figs. 2a and 2e). Occlusal surface oriented anteroposteriorly in same line as lateral edge of rostrum.

P3.—P3 anteroposteriorly elongate, blade-like, and bears 7 buccal and lingual enamel ridgelets ascending anterodorsally from 7 main crest cuspules. Anterior third flexes slightly buccally. P3 bears moderately developed posterolingual eminence. P3 much longer than all molars, equal in length to M1–2 combined (Fig. 2b).

Upper molars.—Bunolophodont. Holotype with M1 slightly worn, dentine of protocone, paracone, and metaconule breached; M2 slightly worn, dentine of paracone breached; M3–4 unworn (Fig. 2b). M1 protoloph and metaloph of equal width. M2–4 protoloph wider than metaloph. Lingual margin of tooth row virtually straight; buccal margin convex laterally due to marked size reduction of molars posteriorly. Paracrista low but distinct, merges with weaker (worn) protocrista to form protoloph. Preprotocrista unites with preparacrista forming precingulum. Postprotocrista weak, unites with strong premetaconulecrista. Metacone higher crowned than metaconule. Metacrista well developed forming majority of metaloph. Metaconulecrista weak. Premetacrista and postparacrista weakly developed and do not unite. Postmetacrista moderately well developed, terminates in position of stylar cusp E. Weak postmetaconulecrista joins postmetacrista at position of stylar cusp E defining posterior border. M4 highly reduced, protocone well-developed, paracone reduced, metacone highly reduced, metaconule absent. Preparacrista forms a small precingulum, paracrista weak, unites with well-developed preprotocrista. Postparacrista runs posterobuccally and contacts metacone, defining posterior border of M4 (Fig. 2b).

Dentary.—Horizontal ramus stout with a convex ventral margin, digastric eminence deep, occurs below m1 hypolophid (depth 8.7 mm; Figs. 2e–j). Digastric sulcus shallow (Figs. 2e and 2j). Buccinator sulcus straight, shallow, extends beneath posterior third of p3 to protolophid of m1. Anterior root of vertical ascending ramus adjacent to posterior of m3 protolophid (Figs. 2f and 2l). Angular process wide; lingual border thickened, tip pointed posteriorly. Masseteric fossa deep, ventral border extends

well below buccinator sulcus to half depth of horizontal ramus. Anterior insertion area for 2nd layer of masseter muscle thin and restricted to rim of masseteric fossa (Figs. 2f and 2l). Masseteric foramen large, anteroventrally oriented and leads into masseteric canal which extends to beneath m1 protolophid. Mandibular foramen oval shaped, opening largely posteriorly (Figs. 2g, 2h, and 2j). Articular process anteroposteriorly wide, articular condyle small, wider laterally. Coronoid process anteroposteriorly wide (viewed laterally), with slight posterior "hook" at dorsal end.

Lower incisor.— Lanceolate i1, bears moderate wear on anterior half of superior border (Figs. 2f and 2l). Diastema short, approximately 2/3 length of p3.

p3.—Blade-like p3 anteroposteriorly elongate, aligned with molar row. Bears 8 buccal and lingual enamel ridges, which descend vertically from 8 crest cuspules. p3 equal in length to m1–2 combined (Figs. 2f–l).

Lower molars.—Bunolophodont. Holotype with m1 slightly worn, dentine of protoconid and hypoconid breached; m2 slightly worn, dentine of hypoconid breached; m3–4 unworn (Figs. 2g and 2k). Lophid faces smooth; m1 protolophid narrower than hypolophid, m2–4 hypolophid narrower than protolophid. Metaconid and entoconid taller than protoconid and hypoconid. Pre- and postmetacristids and pre- and post-entocristids all well developed. Well-developed metacristid forms protolophid, protocristid very weak. Well-developed entocristid forms hypolophid, hypocristid very weak. Low lingual cristid obliqua bisects interlophid valley. Paracristid (buccal) merges with premetacristid enclosing small trigonid basin. Small postcingulid defined by equally developed postentocristid and posthypocristid. Highly reduced m4, metaconid, protoconid, and hypoconid subequal in height, entoconid absent. Weak premetacristid merges with buccal paracristid defining reduced trigonid basin. Weak buccal cristid oblique connects protolophid and hypolophid (Figs. 2g and 2k).

Comparison with Other Species of Bettongia

Cranium.—*Bettongia anhydra* is smaller in overall cranial dimensions than *B. penicillata*, *B. gaimardi*, *B. lesueur*, and *B. tropica*, but larger than *B. pusilla*. Its dentition is larger relative to the size of the cranium than in all other bettongs (although the cranium of *B. pusilla* is unknown; Figs. 3a, 3d, 3g, 3j, and 3m). Compared with the other species of *Bettongia*, *B. anhydra* has a more reduced M4 relative to M3, a shorter rostrum, and narrower frontals and nasals (Table 1; Figs. 2 and 3); interorbital region more constricted than in any other species in the genus (Table 1); braincase narrower and more tapered anteriorly than in other bettongs (Finlayson 1958); squamosal makes greater contribution to the zygomatic arch which is deep and robust than in other *Bettongia* spp. *B. anhydra* shares with *B. lesueur* marked inflation of the tympanic bulla, an attribute that easily distinguishes the crania of these species from those of *B. penicillata*, *B. gaimardi*, and *B. tropica* (Fig. 3). Temporal crests are well developed but instead of following the line of the interorbital ridge they extend dorsally toward the midline of the skull suggesting large temporalis muscles relative to skull size (Fig. 2d); diastema and anterior palatal foramina shorter than in other species of *Bettongia*, the posterior terminus of the latter occurring near the anterior border of the canine; posterior palatal foramina
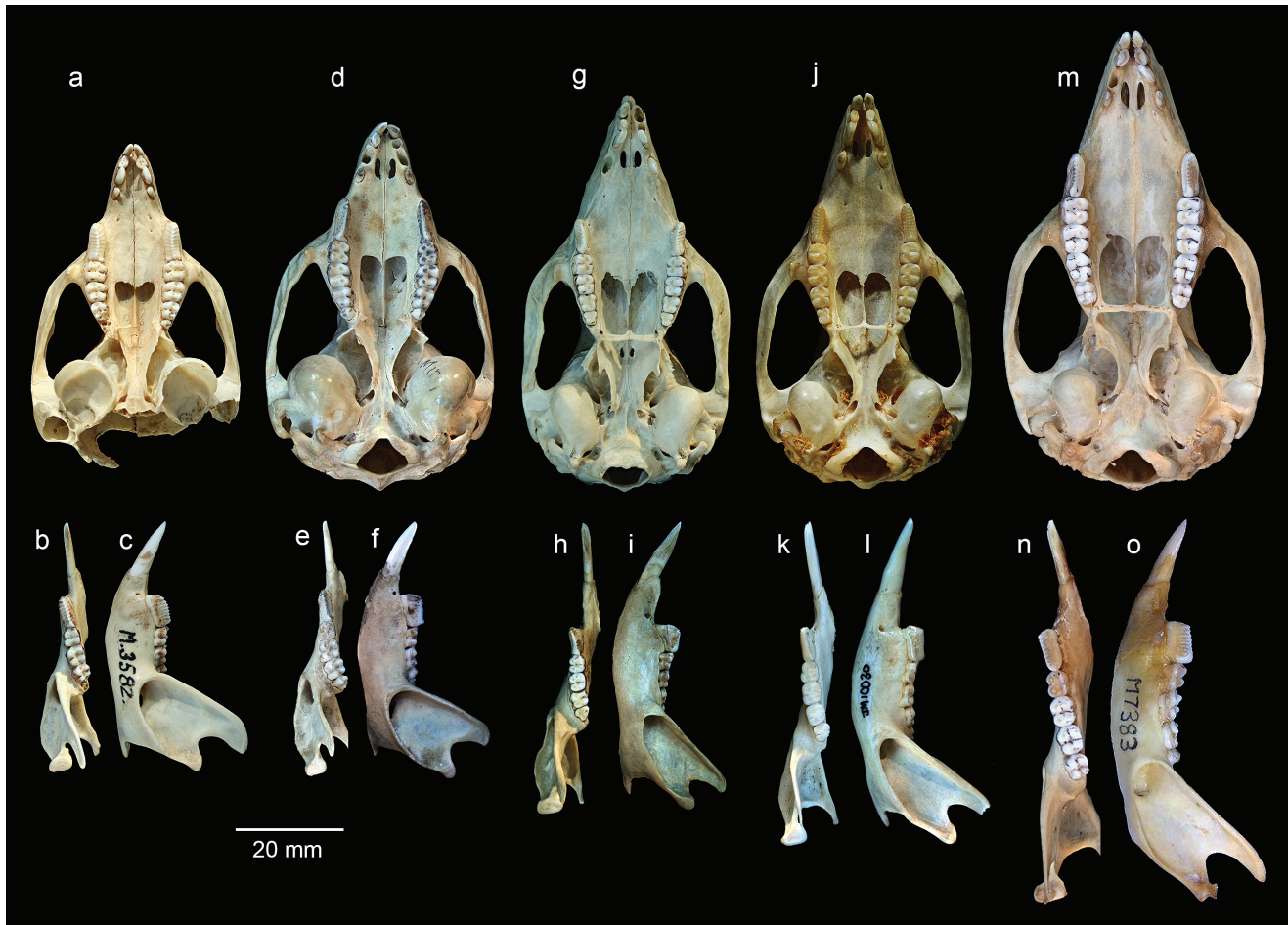
Fig. 3.—Comparison of *Bettongia anhydra* with other extant species of *Bettongia*, showing occlusal view of the skull and left dentary and buccal lateral view of the left dentary of a–c) *B. anhydra*; d–f) *B. lesueur*; g–i) *B. penicillata*; j–l) *B. tropica*; m–o) *B. gaimardi*.

large with anterior margins occurring near the posterior margin of M1 but shorter than in other bettongs (Fig. 3).

P3.—The P3 of *B. anhydra* flexes slightly anterobuccally but remains within the line with the molar row; differs from *B. gaimardi*, *B. lesueur*, *B. moyesi*, *B. pusilla*, and *B. tropica* in which P3 is straight and in line with the molar row (Fig. 2); differs from *B. gaimardi*, *B. lesueur*, and *B. moyesi* in which the lingual face of P3 is convex; differs from *B. penicillata* in which P3 flexes anterobuccally outside the line of the molar row; and differs from that of *B. gaimardi*, *B. lesueur*, *B. pusilla*, and *B. tropica* in which the superior and inferior borders of P3 are subparallel. It is similar to *B. penicillata* in that anterobuccal flexion of P3 increases the depth of the enamel on the anterior buccal face of the tooth such that it is approximately twice as deep as the posterior of the tooth (Wakefield 1967).

Upper molars.—Upper molars of *B. anhydra* differ from all other bettongs in the steepness of the molar gradient and extreme reduction of M4. It further differs from *B. pusilla* in which m1–4 approach equal size and are higher crowned and more lophodont (McNamara 1997); *B. gaimardi* in which M4 is only slightly smaller than M1–3 and in *B. penicillata*, *B. lesueur*, and *B. tropica* in which M1 ≤ M2 > M3 > M4, but M4 is much less reduced (Fig. 3).

Dentary.—Dentaries of *B. anhydra* are short relative to tooth-row length and in lateral view the ascending ramus of *B. anhydra*

obscures the view of m4 and most of m3 (Fig. 3c) In *B. gaimardi* (Fig. 3o), *B. lesueur* (Fig. 3f), *B. penicillata* (Fig. 3i), and *B. pusilla*, the ascending ramus obscures the view of m4 only and in *B. moyesi*, the ascending ramus obscures only part of m4. The dentary of *B. anhydra* also differs from *B. gaimardi*, *B. lesueur*, *B. penicillata*, and *B. pusilla* in the robustness of the horizontal ramus (the ventral margin of the jaw of *B. moyesi* is unknown), the greatest depth of which occurs quite anteriorly at the digastric eminence below m1 (Fig. 3; Finlayson 1957, 1958). It differs from *B. penicillata*, *B. gaimardi*, *B. moyesi*, *B. pusilla*, and *B. tropica* in the proportions of the coronoid process which is long and broad with subparallel borders, and in the angle between the ascending ramus and horizontal ramus which is more acute (Fig. 3).

p3.—p3 of *B. anhydra* (Figs. 2i, 3b, and 3c) has fewer, more broadly spaced cuspules and grooves than seen in *B. lesueur* (Figs. 3e and 3f) and differs from *B. gaimardi* (Figs. 3n and 3o), *B. lesueur* (Figs. 3e and 3f), *B. moyesi*, and *B. tropica* (Figs. 3k and 3l) in that the anterior portion of p3 deflects slightly buccally, though not as much as in *B. penicillata* (Figs. 3h and 3i); differs from *B. gaimardi*, *B. lesueur*, *B. pusilla*, and *B. tropica* in which the superior and inferior borders of p3 are subparallel but is similar to *B. penicillata* in that anterobuccal flexion of p3 increases the depth of the enamel on the anterior buccal face of the anterior portion of the tooth making it slightly deep than in the posterior portion of the tooth (Wakefield 1967).

Lower molars.—Lower molars of *B. anhydra* can be distinguished from other bettongs by their high posterior molar gradient where m1 ≤ m2 > m3 >> m4 and the extreme reduction of m4 (as in upper molars; Fig. 3).

Genetic Analysis

Approximately 200 bp of aDNA were successfully isolated from the cytochrome *b* gene of the *B. anhydra* holotype. Comparison of its DNA sequence with those species of *Bettongia* on GenBank (*B. gaimardi*, *B. lesueur*, *B. penicillata*, and *B. tropica*) revealed that all species share 92% or fewer identical sites in this DNA fragment—a strong indication that it is a genetically distinct species. Phylogenetic analysis (Fig. 4) of this cytochrome *b* fragment grouped *B. anhydra* as sister to *B. lesueur*, but with poor support. Phylogenetic analysis in BEAST was unable to clearly resolve the branching topology between *B. anhydra*, *B. lesueur*, and the other "surface nesting" bettongs. Kimura-2-p pairwise analyses of sequence data determined by MEGA 5.2.2 (Tamura et al. 2011) indicated the genetic distance between *B. anhydra* and other bettongs is estimated to be between 9.6% and 12% for the cytochrome *b* gene. The depth of this genetic split, taken together with the result of the morphological analyses, provides strong support for the specific status of *B. anhydra.*

DISCUSSION

Taxonomy.—Finlayson (1957, 1958) stated that he would have assigned *B. anhydra* specific status if a series of specimens demonstrating its unique attributes existed. The overriding factor that drove Finlayson's placement of *B. anhydra* within *B. penicillata* seems to have been the similarity of their P3. Wakefield (1967), persuaded more by the overall shape of the cranium, placed the Lake Mackay specimen within *B. lesueur*. Aided by the recognition of an additional specimen and DNA analysis,

we clearly show that *B. anhydra* is distinct from all other members of its genus. This is supported by evidence of its former sympatry with both *B. lesueur* and *B. penicillata* which also occupied semi-arid to arid habitats. *B. anhydra* shares several primarily plesiomorphic features with *B. lesueur* and *B. moyesi* suggesting that they lie outside a clade containing the remaining extant species of *Bettongia*, which appear more derived.

Functional adaptations.—Many of the differences distinguishing *B. anhydra* from other bettong species relate to the shortening of the skull, e.g., reduced rostral length, short diastema, short palatal foramina, and highly reduced 4th molars. Mammalian rostrum morphology typically correlates with feeding adaptations (e.g., Mora et al. 2003; Pergams and Lawler 2009; Wilson and Sánchez-Villagra 2010). By shortening the rostrum and dentary but retaining unreduced anterior dentition, *B. anhydra* may have been able to apply greater bite force to its sectorial premolar or anterior molars, potentially allowing it to exploit harder foods such as browse or large seeds. This is consistent with the relatively high positioning of the temporalis origin, which suggests the presence of large temporalis muscles relative to skull size.

Bettongs occupying temperate parts of Australia are primarily fungivores (Johnson and McIlwee 1997; Claridge et al. 2007). However, *B. lesueur*, the most arid-adapted extant bettong, subsists mainly on roots and tubers, also occasionally consumes bulbs, carrion, insects, and seeds, including those of the Quandong and Sandalwood (*Santalum* spp.), which have hard seed-coats (Claridge et al. 2007). *Caloprymnus campestris*, a bettongin which occupied the absolutely lowest rainfall zone in Australia prior to its extinction near the middle of the 20th century, also had a very short robust skull and is reported to be have been primarily herbivorous (Finlayson 1932). Although hypogeal fungi occur in the Australian arid zone (Trappe et al. 2008), the morphological similarities shared by *B. anhydra*, *B. lesueur*, and *C. campestris* suggest that *B. anhydra* may have supplemented its diet with browse. A similar diet was inferred for *Borungaboodie hatcheri*, a very large bettong known only from the late Pleistocene of southwestern Australia (Prideaux 1999).

The most striking characteristic shared by *B. lesueur* and *B. anhydra* is the extreme inflation of their auditory bullae. Desert dwelling mammals frequently possess more inflated auditory bullae than similar-sized forest-dwelling relatives. A larger middle ear air volume is often associated with more acute low frequency hearing which may enhance predator detection, thereby conferring advantages to animals foraging in open areas (e.g., Francescoli et al. 2012). Phylogenetic analysis (Fig. 4) identified *B. lesueur* and *B. anhydra* as sister taxa. Therefore, it is possible that inflated auditory bullae occurred in a common ancestor as an early adaptation to aridification of Australia.

Ecological implications.—The near obliteration of bettongs from mainland Australia has likely had serious ecological repercussions. Bettongs, potoroos, and similar ground-foraging small mammals cultivate the soil and in doing so provide important ecological services (Fleming et al. 2013; McDowell 2014). Soil disturbance has implications for incorporation of organic matter, aeration, moisture infiltration, seed germination, and seedling establishment (Martin 2003; Fleming et al. 2013). In addition, it promotes microorganism growth, influences topsoil formation,
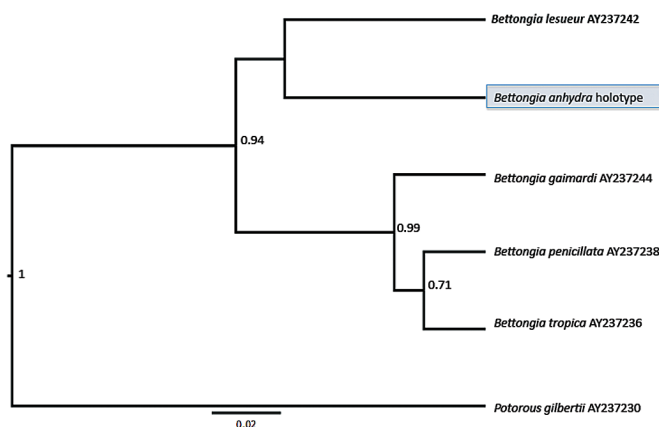

Fig. 4.—Bayesian phylogeny showing relationships between *Bettongia anhydra* (highlighted) and all other extant *Bettongia* species. Species are labeled with GenBank accession numbers. This tree was generated in BEAST using 203 bp of cytochrome *b* gene. A Hasegawa, Kishino, and Yano model and births-deaths tree prior with invariant gamma substitution sites was imposed with a relaxed molecular clock. Posterior probabilities > 70% are shown on selected nodes, scale bar represents the number of substitution sites per year.

and improves water penetration and retention, thereby enhancing soil structure (Fleming et al. 2013). Bettongs also play an integral role in the dispersal of seeds and fungal spores, many of which form symbiotic relationships crucial for the establishment and growth of numerous native plants, particularly eucalypts (Claridge et al. 2007). These ecological services are not replicated by introduced fossorial mammals such as the European rabbit, *Oryctolagus cuniculus* (James et al. 2011). Ecological services performed by bettongs are so important that they may actually determine vegetation succession and facilitate greater biodiversity (Martin 2003). The loss of bettongs and other ground-foraging small mammals from much of mainland Australia has probably compounded soil compaction problems caused by hard-hooved livestock, leaving little doubt that their loss will have far-reaching ecological impacts (e. g., Johnson and McIlwee 1997; Garkaklis et al. 1998; Martin 2003).

Since Europeans colonized Australia every bettong species, and most other potoroines, have either been extirpated from most of their original geographic range or driven entirely to extinction (see van Dyck and Strahan 2008). *Bettongia gaimardi gaimardi* is restricted to Tasmania and the mainland form *B. gaimardi cuniculus* is extinct. *Bettongia lesueur*, which once occupied much of the continents arid and semi-arid zones only a century ago, is now restricted to a few small islands off the Western Australian coast (Burbidge et al. 2007). *Bettongia penicillata ogilbyi* persists in a few small populations in southern Western Australia but *B. p. penicillata* is extinct. *Bettongia tropica* persists in a very small part of Queensland (see van Dyck and Strahan 2008). *Bettongia pusilla*, known exclusively from Holocene Nullarbor Plain cave accumulations (McNamara 1997), may have become extinct prior to European colonization of Australia. However, given the isolated nature of its predicted range, it is possible it persisted unnoticed until the arrival of Europeans before succumbing to the combined impacts of European-led habitat destruction and introduction of exotic predators and competitors. The evidence for such extinction pressures are stronger for *B. anhydra*, given that it survived in central Australia well into the 1930s. Its disappearance, along with many other small- to medium-sized Australian mammals, coincides with the 4th toll of the post-European mammal extinction bell (Johnson 2006:171–172).

All species of *Bettongia* appear to be highly sensitive to anthropogenically driven environmental change. The recognition of yet another recently extinct Australian mammal suggests that the extent of Australian biodiversity loss since Europeans settlement may be greater than previously thought. This research also highlights the potential that numerous cryptic or rare species may remain hidden among their more common, morphologically similar relatives. However, the loss of ecological services that accompanied the extirpation or extinction of bettongs and other digging mammals may be of greater ecological importance. Given the unlikelihood that any extant species of bettong will be restored to its former range and abundance, the loss of these landscape engineers and the ecological services that they once performed will make the restoration of Australia's pre-European ecology all the more difficult.

LITERATURE CITED

BURBIDGE, A. A., J. SHORT, AND P. J. FULLER. 2007. Relict *Bettongia lesueur* warrens in Western Australian deserts. Australian Zoologist 34:97–103.

CALABY, J. H., AND B. J. RICHARDSON. 1988. Potoroidae. Pp. 53–59 in Zoological catalogue of Australia. 5. Marsupialia (D. W. Walton, ed.). Australian Government Publishing Service, Canberra, Australia.

CLARIDGE, A. W., J. H. SEEBECK, AND R. ROSE. 2007. Bettongs, potoroos and the musky rat-kangaroo. CSIRO Publishing, Collingwood, Australia.

DESMAREST, A. G. (1822). Description of Kangurus gaimardi. Mammalogie ou description des espèces de mammifères. Pp. 542 in Encyclopédie Methodique (Dictionnaire Encyclopédique Méthodique) (A. G. Desmarest, ed.). Supplement ii V. Agasse, Paris, France.

DRUMMOND, A., ET AL. 2011. Geneious v5. 4. http://www.geneious.com/. Accessed 21 January 2012.

DRUMMOND, A. J., AND A. RAMBAUT. 2007. BEAST: Bayesian evolutionary analysis by sampling trees. BMC Evolutionary Biology 7:214.

DRUMMOND, A. J., M. A. SUCHARD, D. XIE, AND A. RAMBAUT. 2012. Bayesian phylogenetics with BEAUti and the BEAST 1.7. Molecular Biology and Evolution 29:1969–1973.

ELDRIDGE, D. J., AND A. I. JAMES. 2009. Soil-disturbance by native animals plays a critical role in maintaining healthy Australian landscapes. Ecological Management and Restoration 10:S27–S34.

ELDRIDGE, D. J., T. B. KOEN, A. KILLGORE, N. HUANG, AND W. G. WHITFORD. 2012. Animal foraging as a mechanism for sediment movement and soil nutrient development: evidence from the semi-arid Australian woodlands and the Chihuahuan Desert. Geomorphology 157:131–141.

FINLAYSON, H. H. 1932. *Caloprymnus campestris*. Its recurrence and characters. Transactions of the Royal Society of South Australia 56:148–167.

FINLAYSON, H. H. 1957. Preliminary description of two new forms of *Bettongia* (Marsupialia). The Annals and Magazine of Natural History 10:552–554.

FINLAYSON, H. H. 1958. On central Australian mammals (with notice of related species from adjacent tracts). Part III – the Potoroinae. Records of the South Australian Museum 13:235–302.

FLANNERY, T. F., AND M. ARCHER. 1987. *Bettongia moyesi*, a new and plesiomorphic kangaroo (Marsupialia: Potoroidae) from Miocene sediments of northwestern Queensland. Pp. 759–767 in Possums and opossums: studies in evolution (M. Archer, ed.). Surrey Beatty and Sons, Sydney, Australia.

FLEMING, P. A., H. ANDERSON, A. S. PRENDERGAST, M. R. BRETZ, L. E. VALENTINE, AND G. E. HARDY. 2013. Is the loss of Australian

digging mammals contributing to a deterioration in ecosystem function? Mammal Review 44:94–108.

FRANCESCOLI, G., V. QUIRICI, AND R. SOBRERO 2012. Patterns of variation in the tympanic bulla of tuco-tucos (Rodentia, Ctenomyidae, *Ctenomys*). Acta Theriologica 57:153–163.

GARKAKLIS, M. J., J. S. BRADLEY, AND R. D. WOOLLER. 1998. The effects of Woylie (*Bettongia penicillata*) foraging on soil water repellency and water infiltration in heavy textured soils in southwestern Australia. Australian Journal of Ecology 23:492–496.

GRAY, J. E. 1821. On the natural arrangement of vertebrose animals. London Medical Repository 15:296–310.

GRAY, J. E. 1837. Description of some new or little known Mammalia, principally in the British Museum collection. Magazine of Natural History 1:577–587.

HAOUCHAR, D., J. HAILE, P. B. S. SPENCER, AND M. BUNCE. 2013. The identity of the Depuch Island rock-wallaby revealed through ancient DNA. Australian Mammalogy 35:101–106.

JAMES, A. I., D. J. ELDRIDGE, T. B. KOEN, AND K. E. MOSEBY. 2011. Can the invasive European rabbit (*Oryctolagus cuniculus*) assume the soil engineering role of locally-extinct natives? Biological Invasions 13:3027–3038.

JOHNSON, C. 2006. Australia's mammal extinctions: a 50,000 year history. Cambridge University Press, Melbourne, Australia.

JOHNSON, C., AND A. MCILWEE. 1997. Ecology of the northern bettong, *Bettongia tropica*, a tropical mycophagist. Wildlife Research 24:549–559.

MARTIN, B. G. 2003. The role of small ground-foraging mammals in topsoil health and biodiversity: implications to management and restoration. Ecological Management and Restoration 4:114–119.

MCDOWELL, M. C. 2014. Holocene vertebrate fossils aid the management and restoration of Australian ecosystems. Ecological Management and Restoration 15:58–63.

MCDOWELL, M. C., A. BAYNES, G. C. MEDLIN, AND G. J. PRIDEAUX. 2012. The impact of European colonization on the late-Holocene non-volant mammals of Yorke Peninsula, South Australia. The Holocene 22:1441–1450.

MCNAMARA, J. A. 1997. Some smaller macropod fossils of South Australia. Proceedings of the Linnean Society of New South Wales 117:97–106.

MORA, M. A., I. OLIVARES, AND A. I. VASSALLO. 2003. Size, shape and structural versatility of the skull of the subterranean rodent *Ctenomys* (Rodentia, Caviomorpha): functional and morphological analysis. Biological Journal of the Linnean Society 78:85–96.

OWEN, R. 1866. On the anatomy of vertebrates. Longmans, Green and Co., London, England.

PERGAMS, O. R. W., AND J. J. LAWLER. 2009. Recent and widespread rapid morphological change in rodents. PloS One 4:e6452.

POSADA, D. 2008. jModelTest: phylogenetic model averaging. Molecular Biology and Evolution 25:1253–1256.

PRIDEAUX, G. J. 1999. *Borungaboodie hatcheri* gen. et sp. nov., a very large bettong (Marsupialia: Macropodoidea) from the Pleistocene of southwestern Australia. Records of the Western Australian Museum Supplement No. 57:317–329.

PRIDEAUX, G. J. 2004. Systematics and evolution of the sthenurine kangaroos. University of California Publications in Geological Sciences 146:1–623.

PRIDEAUX, G. J., AND N. M. WARBURTON. 2010. An osteology-based appraisal of the phylogeny and evolution of kangaroos and wallabies (Macropodidae: Marsupialia). Zoological Journal of the Linnean Society 159:954–987.

QUOY, J. R. C., AND J. P. GAIMARD. 1824. Zoologie. Pp. 712 in de Voyage Autour du Monde, ... exécuté sur les corvettes de S.M. 1'Uranie et la Physicienne pendant les années 1817, 1818, 1819 et 1820. Vol. 1 iv. (L. C. D. Freycinet, ed.). Chez Pillet Aîne, Paris, France.

RAMBAUT, A. 2007. FigTree, a graphical viewer of phylogenetic trees. http://tree.bio.ed.ac.uk/software/figtree. Accessed 21 January 2012.

RAMBAUT, A., AND A. DRUMMOND 2009. Tracer version 1.5. 0. http://tree.bio.ed.ac.uk/software/tracer/. Accessed 21 January 2012.

SEEBECK, J. H., AND R. W. ROSE. 1989. Potoroidae. Pp. 716–739 in Fauna of Australia 1B Mammalia (D. W. Walton and B. J. Richardson, eds.). Australian Government Publishing Service, Canberra, Australia.

SHORT, J. 1998. The extinction of rat-kangaroos (Marsupialia: Potoroidae) in New South Wales, Australia. Biological Conservation 86:365–377.

TAMURA, K., D. PETERSON, N. PETERSON, G. STECHER, M. NEI, AND S. KUMAR. 2011. MEGA5: molecular evolutionary genetics analysis using maximum likelihood, evolutionary distance, and maximum parsimony methods. Molecular Biology and Evolution 28:2731–2739.

TRAPPE, J. M., A. W. CLARIDGE, D. L. CLARIDGE, AND L. LIDDLE. 2008. Desert truffles of the Australian outback: ecology, ethnomycology, and taxonomy. Economic Botany 62:497–506.

VAN DYCK, S., AND R. STRAHAN. 2008. The mammals of Australia. 3rd ed. Reed New Holland, Sydney, Australia.

VITOUSEK, P. M. 1990. Biological invasions and ecosystem processes: towards an integration of population biology and ecosystem studies. Oikos 57:7–13.

WAKEFIELD, N. A. 1967. Some taxonomic revision in the Australian marsupial genus *Bettongia* (Macropodidae), with description of a new species. Victorian Naturalist 84:8–22.

WILSON, L. A. B., AND M. R. SÁNCHEZ-VILLAGRA. 2010. Diversity trends and their ontogenetic basis: an exploration of allometric disparity in rodents. Proceedings of the Royal Society of London, B. Biological Sciences. 277:1227–1234.

WISELY, S. M., J. E. MALDONADO, AND R. C. FLEISCHER. 2004. A technique for sampling ancient DNA that minimizes damage to museum specimens. Conservation Genetics 5:105–107.

APPENDIX I

Specimens used for comparison with *Bettongia anhydra*. Bold denotes specimens that were sympatric with *B. anhydra* specimens.

Bettongia gaimardi Desmarest, 1822: SAM M7386, M7387, M7388.

Bettongia lesueur Quoy and Gaimard, 1824: FUR 034 (Holocene fossils from Corra-Lynn Cave, Yorke Peninsula, South Australia); SAM M1702, M10769.

Bettongia penicillata Gray, 1837: FUR 011, 031; SAM M6211, M11247; WAM 66.1.7c, 66.6.58, 66.12.4a, 66.12.4b, 66.12.11, 67.3.54, 67.3.98, 67.5.1, 67.5.4, 67.5.41–.44, 67.8.69, 67.10.193,

67.10.194, 67.10.31, 67.10.324, 67.10.360, 67.10.37, **67.10.523-.525**, 68.2.90, 68.2.91, 68.3.17, 69.7.649, 69.7.655, 69.7.661, 70.5.22, 70.5.23, 71.9.36, 72.1.109, 72.1.139, 72.1.199, 72.1.224, 72.1.467, 72.1.489a, 72.1.489b, 72.1.634a, 72.1.634b, 72.1.676, 72.1.776, 72.1.777, 72.1.778, 72.1.800, 72.1.824, 72.1.845-.847, 72.1.898a, 72.1.898b, 72.1.924, 72.1.1104, 72.1.1105, 72.6. 184, 75.12.21, 76.4.35.

Bettongia pusilla McNamara, 1997: SAM P35442, P35446, P35450, P35451; WAM 67.10.227, 67.10.412, 68.3.5, 71.1.29a, 72.1.108, 72.1.822, 72.1.823, 76.10.413.
Bettongia tropica Wakefield, 1967: MV C6870, AMNH 65279, QM M10030.